JAST, Vol. 2, No. 2, pp 19–27

JAST
Journal of Aerospace Science and Technology

Physical Simulation of Baroclinic Waves and Vortices in The Atmosphere

A. A. Bidokhti[1], I. Babaeian[2]

Atmospheric flows are often associated with long waves which, in the presencet of fronts (regions with large spatial gradients of temperature or density) can produce vortices as a result of instability. Vortex motion also can lead to front formation. These processes are often associated with potential vorticity advection, which is nonlinear and, hence, not easily computable. Laboratory experiments (physical simulation) can help us to understand such complex processes in atmosphere and ocean.

We present some laboratory experiments in a rotating fluid in which temperature (or density) gradients are imposed producing wavy circulations that can, under certain conditions, become unstable and result in vortices. One of the experiments involves rotating annulus in which a circular layer of uniform depth is subjected to a radial temperature gradient. Thermal Rossby and Taylor number values similar to those in large scale atmospheric flows are chosen for these experiments. The results show that baroclinic instability can produce wavy motion, which grows and produces flow pattern as well as vortices which are comparable to the atmospheric flow pattern. In another experiment, a baroclinic vortex is produced by injecting a buoyant fluid on the free surface of a denser layer of fluid (usually satlier water) in solid-body rotation. Flow visualization and measurement show that for a relatively small source Froude number when the size of the vortex is about four times the internal Rossby radius of deformation of the environment, the vortex goes unstable and usually turns in two vortices (with circumferential wave number 2) and some of the potential energy of the flow is released into the kinetic energy of the flow. Such behavior is also observed in the polar stratospheric vortex, which has implications for the formation of ozone hole in polar atmosphere.

INTRODUCTION

Large-scale flows in the atmosphere and ocean as general circulation systems often go through instability and form wavy motions and vortices that are associated with potential energy release. They have a key role in the meridian transportation of momentum and heat in the atmosphere. The atmospheric eddies superimposed on mean zonal flows are often associated with fronts that, as they pass over a region, can determine the weather that we depend on nowadays. Hence understanding these processes are very important for more accurate weather prediction, which is done using numerical methods involvesing solutions of governing equations with proper boundary conditions.

Extensive physical simulations of global circulation of the atmosphere has been carried out by Hide [1, 2 and 3] using laboratory experiments. He has simulated various regimes of the atmospheric-like motions in a rotating annulus by changing the Rossby and Taylor numbers (see section 3), and found that as these numbers increase together with radial temperature gradient (as pole-equator temperature difference in the atmosphere) with a given rotation, the flow goes through a zonal symmetry, wavy (Rossby waves) zonal flow and then zonal-wave flow, with eddies that are produced by hydrodynamic instability. Such flow patterns are often observed in the atmosphere (figure 1)

1. *Geophysics Institute of Tehran University, Tehran, I.R. Iran*
2. *National Institute of Climatology, 91735-491, Mashhad, I. R. Iran*

which indicates that the mass (temperature field) of the atmosphere is far from equilibrium and continuously goes through instability in which the potential energy is converted to motions as waves and eddies. Such motions are also known as the sloped convection [1]. Recently Tajima [4] studied the baroclinic instability in a rotating fluid using careful flow visualization and revealed the 3d structure of the baroclinic vortex in a rotating differentially heated annulus. Experiments by Bastin and Read [5] on rotating annulus with internal heating also have revealed baroclinic wave structure similar to the one observed in the atmosphere of the giant planet Jupiter.

The theoretical and laboratory studies of the baroclinic vortices have been carried out by Lindon and Hapfinger [6 and 7]. These include the way baroclinic vortices interact with each other creating highly non-linear chaotic behaviors. The authors have also looked at the way the vortices can exchange their energy with the mean flow. Bidokhti and Tritton [8] studied barotropic vortices showing that when the absolute vorticity (sum of relative and background vorticity) is positive, the flow is more stable, and vortices lose energy to the mean flow. Usually waves and vortices have two-dimensional structures in the atmosphere. In such flows vorticity vector is coincided with background vorticity. In this case, rotation increases the stability of the vortex and the transportation of energy reduces from mean flow to the perturbed flow, so the energy of the vortex is transported into the mean flow gradually [1,7]. These studies are important in understanding the large scale atmospheric flows behavior and their prediction. Eddies close streamlines and, therefore, can transport mass, heat and potential vorticity. Hence as they propagate, they can continue to mix in large horizontal distances. In polar regions, in which cold air often sinks, large vortex are formed due to the Coriolis effect. Polar stratospheric air also has strong meridian temperature gradients, which through thermal wind effect [9] can sustain a strong zonal jet encompassing the large polar vortex. It is now known that if this vortex is stable long enough (as in the case of South Pole), it can separate the air inside from the rest of atmosphere, and the temperature inside the vortex can drop dramatically to 180 K, which is suitable for the formation of polar stratospheric clouds that have a dramatic destructive effect on ozone in the polar air (e. g. Turco [10]). Hence the behavior of this polar stratospheric vortex is important for understanding the extension and duration of ozone hole in the southern hemisphere. In this paper we first present results from a laboratory simulation of atmospheric circulation in a dynamic state close to the present atmospheric general circulation state, and look at the behavior of the flow while comparing it with middle latitude flow patterns. In a second experiment, we produce a baroclinic vortex by injecting a buoyant fluid at the free surface of a denser (usually saltier water) layer of fluid in solid-body rotation. The behavior of the vortex is studied using flow visualization and measurements. They are not intended to cover a large parameters range but those associated with some of the features of the real atmosphere.

BAROCLINIC INSTABILITY

In a thermally stratified flow, with gosestrophic motion(with Coriolis-pressure gradient balance), when the isothermal surfaces are inclined large enough, the potential energy of the system can be released and turned into kinetic energy. The release of potential energy is associated with instability of large scale flows in the atmosphere. Due to the meridian gradient of temperature in the atmosphere, the mean flow is in thermal winds balance such as in jet streams existing in the middle latitudes. These flow patterns are often unstable when the horizontal temperature gradient becomes large and perturbations can grow as they have different phase speeds with height and have baroclinic structures. Eady studied the instability of stratified flow in the vertical direction between the z=0 and z=H surfaces ignoring the variation of the Coriolis parameter. Based on this theory, the disturbance with maximum instability has a wavelength which is given by:

$$\lambda_{max} \approx 3.9 L_r \tag{1}$$

where, L_r is the Rossby radius of deformation and is given by:

$$L_r = N\lambda / f \tag{2}$$

where $N=[(g/\theta_o)\partial\theta/\partial z]^{1/2}$ with $\partial\theta/\partial z$ as the vertical potential temperature gradient, is the buoyancy frequency, λ is the vertical wavelength (inverse of the vertical wave number) of disturbance and $f = 2\Omega$ is the background vorticity [9, 11, 12 and13]. L_r is estimated to be about 50 km in the ocean and 1000 km in the atmosphere for typical N, which is about 0.01 s^{-1} for both. These are surprisingly similar to the observed scales of eddies in the ocean and atmosphere respectively. Here we also use similar criteria for the instability of baroclinic vortex going through instability in laboratory experiment.

SIMULATION OF THERMAL ROSSBY WAVES

There are many wave-like features in temperature and geopotential height fields in daily weather charts. The wavelength of these waves is about 4000 km in the atmosphere and 200km in the ocean. Although the beta effect helps the formation of these waves, it

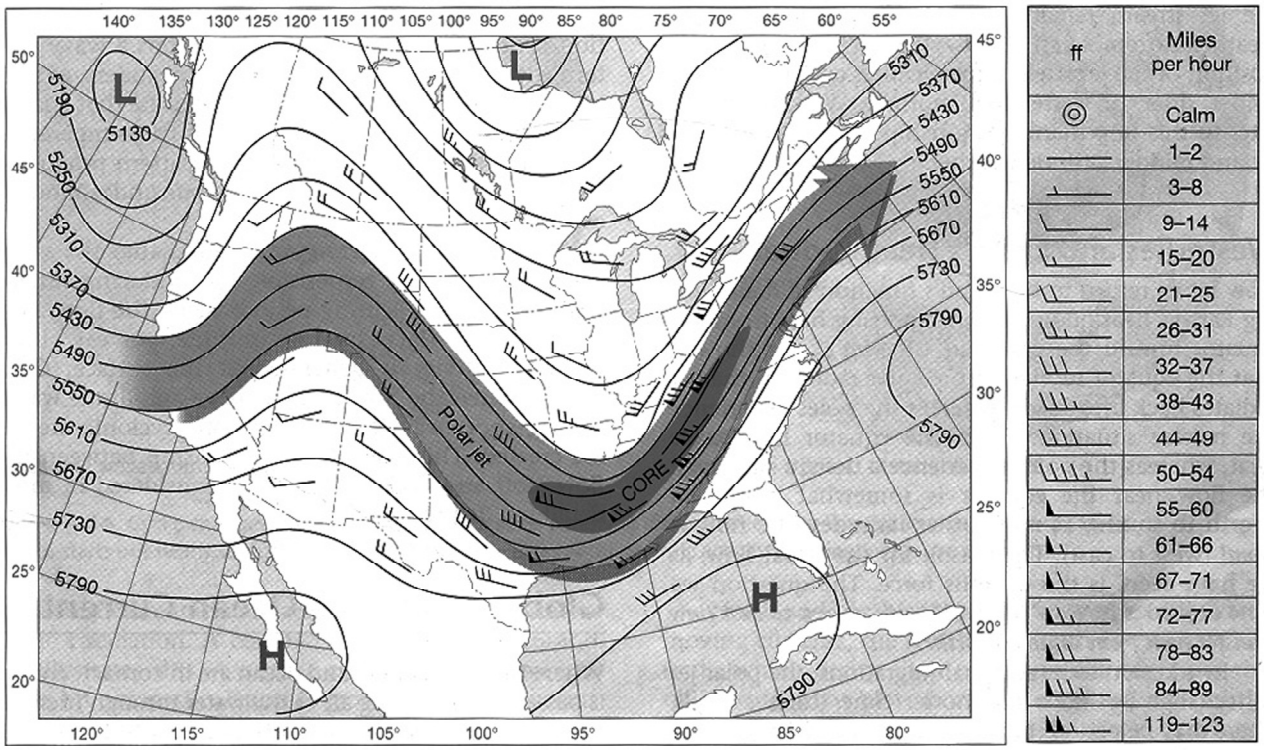

Figure 1. An example of a wave like features and vortices in daily weather charts. The position of the jet stream is shown with a thick arrow.

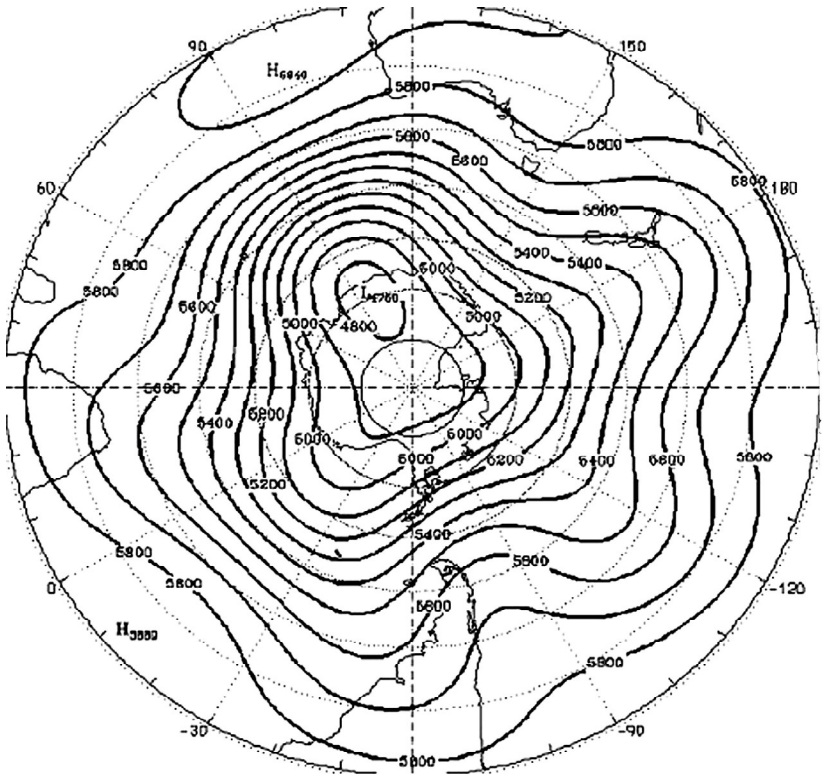

Figure 2. Streamline pattern of air flow on the 500 milibar isobar surface (about middle troposphere) for 25 April 2003 over the southern hemisphere. [Australian Bureau of Meteorology].

has a lesser role in their development. Because of the meridian temperature gradient these long waves have a baroclinic structure as shown in Figure 1 [6 and 13]. These long waves are particularly visible on hemispheric weather charts such as the one shown in Figure 2 for the southern hemisphere. Due to less complicated land and sea cover compared with the northern hemisphere, the flow is more symmetric. The flow pattern is on the 500 mb (almost middle troposphere) showing wavy structure with azimuthal wave number of 5.

A rotating annulus designed at the Geophysical Fluid Laboratory of the Geophysics Institute of Tehran University was used to simulate the atmospheric flow for dimensionless parameters similar to those of real atmosphere. The experiments are meant to generate Rossby waves and circulation as in General Circulation Model (GCM). The annulus consists of three concentric cylinders filled with water of different temperatures, as shown in Figure 3. The working fluid is also water and is in the middle annulus. T_i, T_b and T_a represent temperatures of working water in the middle, outer and inner cylinders respectively. Usually the temperatures are chosen so that $T_a < T_i < T_b$. [1, 2, and 3].

For Ω=0, because of radial temperature gradient, a meridian flow, like Hadley cell was produced in working water. The downdraft of fluid near the cold wall, and the updraft near the surface of the warm wall occurred in the annulus. The meridian speed became faster and faster as the radial temperature gradient increased and the vorticity vector becomes completely zonal as the vertical component of vorticity vanishes.

For $\Omega \neq 0$ the vorticity vector gradually tended to become vertically up to coincide with background vorticity of the annulus. Based on the thermal Rossby number and Taylor number various regimes of waves formed in the annulus:

$$Ro_t = \epsilon g H \delta T / [4\Omega^2 (b-a)^2]$$

$$\tau = 4\Omega^2 (b-a)^5 / (H\upsilon^2) \qquad (3)$$

Where ϵ is the thermal expansion coefficient, δT (typically 20 K) the value of radial temperature

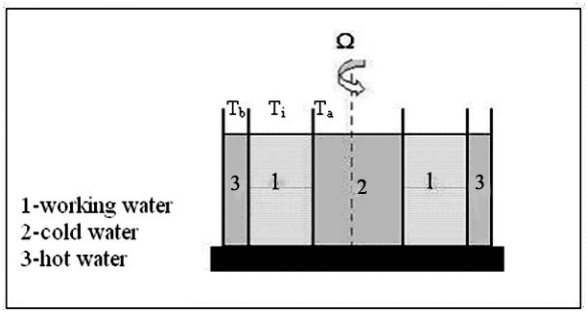

Figure 3. Vertical cross section of the rotating annulus experiment

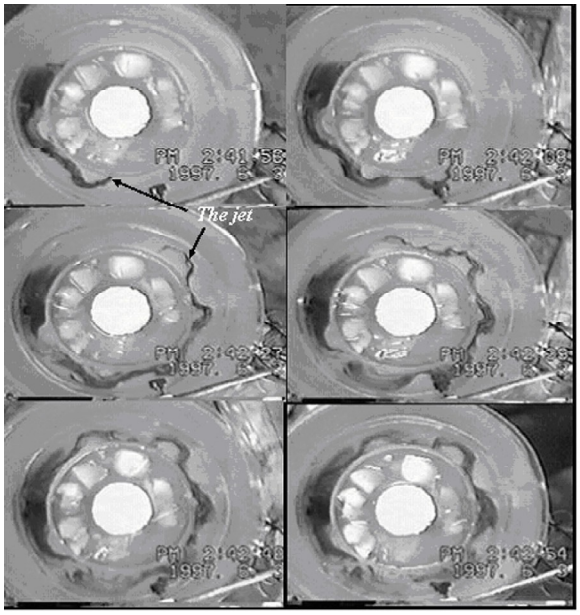

Figure 4. A sequence of photographs of the flow of thermal Rossby wave in the laboratory model with Ro_t>0.4 and $\tau \sim 10^8$. They are taken from the top with a camera attached to the rotating frame. Notice that the jet is meandering jet which revealed by dye release a few seconds before the first photo.

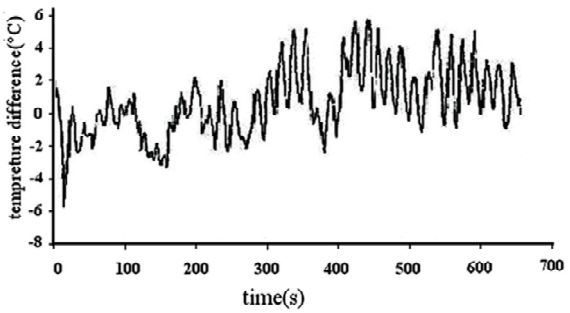

Figure 5. Temperature variation during the formation of Rossby wave (2.5 rad/s, δT~ 25 C)

difference across the annulus, Ω (2.5 rad/s) the rotation rate of system, b-a (0.05 m) is the distance between inner and outer cylinder (working region), H (0.25 m) the depth of the fluid and finally ν (10^{-6} m^2/s) is the coefficient of fluid viscosity. Typically we choose Ro_t>0.4 and $\tau \sim 10^8$. Figure 4 shows the flow visualization of the wavy zonal flow with zonal wave number 8. Small scale mixing is also seen at the edge of jet- stream flow like structure, as observed in the real atmosphere (Figure 1). The time of the dye release is a few seconds before the first image. The jet appears to propagate cyclonically (in the direction of rotating table which is anticlockwise in this case). There is another zonal jet in the lower part of the annulus, which moves in the opposite direction with much smaller speed due to the lower boundary layer,

but it is not visible in these photos as the upper jet has covered the whole annulus.

The time variation of the temperature difference between that recorded from the temperature sensor in the middle of the annulus and the mean temperature is shown in Figure 5. The record shows a wavy nature of temperature field with mainly short and long period harmonics. It also has a harmonic with a very long period comparable to the whole the record length. These are due to the wave-eddy flow passing the probe as the flow structure is advecting the measuring point. Typically they are 10, 100 and 1000 seconds. Such a spectrum of flows also exists in the atmosphere which are known as micro-, meso- and macro- scales typically in order of hours, days and weeks.

We also studied the different patterns in the 500 mb meteorological chart and found that if the Ro_t >0.35, the regular pattern of Rossby waves may break down into irregular waves and subsequent cyclones [9 and 14].

SIMULATION OF THE ATMOSPHERIC BAROCLINIC VORTICES

In a second experiment, the dynamic behavior of a baroclinic eddy was studied. A cylinder filled with denser (saltier) water to a depth of 25 cm was set to rotate on a rotating table to reach a constant solid-body rotation state. The rotation rate was 2.5 rad/s. The radius and height of the cylinder was 30 cm each. When the fluid reached solid body rotation, the fresh colored water was added slowly to the top surface center of the rotating fluid layer (water). Due to the buoyancy force, the fresh water flowed radically on the surface of dense water at the center first. But conservation of potential vorticity in the absence of viscous effect of the fluid leads to clockwise (anticyclonic) rotation of buoyant fluid. Then gradually a vortex with an inverse conic shape was formed near the top of dense water (Figure 6). The initial potential vorticity before adding pure and colored water is f/H and $(f+\zeta)/(H-\eta)$ after adding the water, where f is the background vorticity of the turn table, ζ is the induced relative vorticity by fresh water, H is the total depth of dense water and η is the depth of vortex bottom boundary. As the fresh fluid enters the center of the tank with a constant small rate it initially spread radially outwards due to buoyancy. As a result of angular momentum conservation and in the absence of viscous effect the fluid turns ant cyclonically around the source. The flow in the vortex is then under the balance of Coriolis force (towards the source) and the buoyancy (sloping

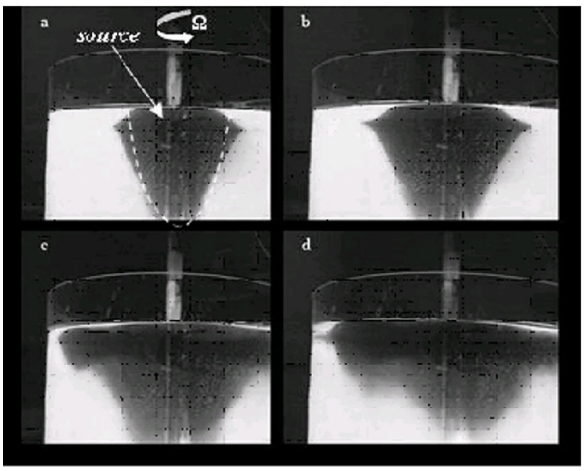

Figure 6. Side view photographs of the vortex before (a, b) and after (c, d) the break up. The photos are taken by the camera attached to the rotating frame. The position of the source is also indicated. In this experiment the density difference is 10 gr/lit, Ω=2.5 rad/s, H=25 cm and L_r =3.05 cm. Theoretical solution of the sloping interface (eq. 5) is also shown in (a) as broken line.

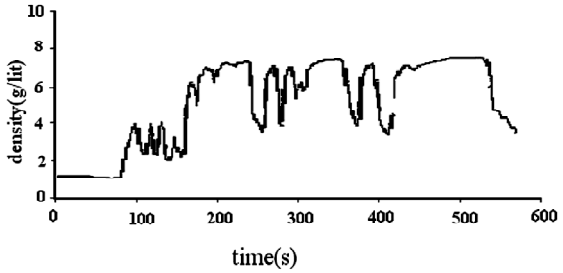

Figure 7. Density records from the sensor initially inside the main vortex which was located at a depth of 5cm and radius of 2 cm from the center of vortex, showing the growth of the instability of the vortex.(In this case L_r=3.75 cm).

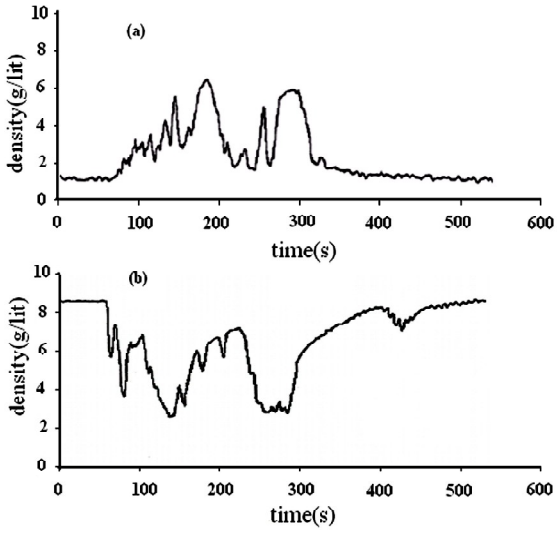

Figure 8. Density records from (a) the sensor initially inside the main vortex, located at a depth of 5cm and radius of 2 cm from the center of the vortex; and (b) the sensor outside the vortex located at a depth of 5cm and radius of 3 cm from the center of vortex showing the growth of the instability and the density structures of the resulting vortices. In this case L_r=5.3 cm).

density interface) radially outward with an azimuthal speed of v_1=-(1/2)fr, where r is the radial distance from the source. The sloping interface is between the deepest center part of the vortex and the vortex surface boundary at which it intersects the surface and forms a surface front. The cyclostrophic balance is then given by:

$$f(v_1 - v_2) + (v_1^2/r) - (v_2^2/r) = g'(ds/dr) \quad (4)$$

where v_2 is the speed of the lower layer and the ds/dr is the slope of the sloping interface and g'=($\delta\rho/\rho$)g is the reduced gravity with $\delta\rho$ being the density difference between the buoyant fluid of the vortex and lower denser fluid. It can be shown that the position of the sloping interface can be found as (Linden, [6]):

$$s(r,t) = h(t) - H[I_o(r/L_r) - 1]/(I_o(R/L_r)) \quad (5)$$

where h(t) is the maximum depth occurring at r=0, R is the radius of vortex, L_r =(g'H)$^{1/2}$/f is the Rosbby radius of deformation of the environment and I_o is the modified Bessel function of the first kind with zero order and f=2Ω. The solution of (5) is indicated in Figure 6(a). The Froude number of the source with a volume flow rate of Q and source area size of A and Rossby number of vortex are respectively Fr= (Q/A)/(g'H)$^{1/2}$ and Ro=(Q/A)/(2ΩR) which are respectively about 0.2 and 0.01 for these experiments, hence rotational effect is strong. As the vortex grows gradually and reaches a certain size, the instability sets in near the sloping interface. At this stage some eddies are developed due to insatiability with some smaller scale mixing. For large-scale flows, the eddy can produce a frontal zone or gravity currents which are often observed in the ocean and atmosphere [6]. To investigate the breaking process of a vortex, we examined various densities of the working water with different rotation rates. Figure 6 presents a sequence of photographs showing the vortex before (a, b) and after (c, d) the breaking process. When the size of the vortex reaches a certain size, about 8 times the Rossby radius of deformation, it starts to oscillate. As the perturbations grow, it breaks up into two smaller vortices having an S-shape structure from the top, with some smaller scale mixing at the edges. The depth of the main vortex is also substantially reduced and hence potential energy is released.

We also put two salinity sensors radially near the boundary of the vortex with one fixed inside the vortex, and the other one in the outer side of the vortex. A data-logger connected to a personal computer was used to record the density data of these sensors. Figure 7 shows an example of the density record from the probe inside the vortex , which shows the onset of the instability and the development of smaller scale eddies as the vortex breaks in two smaller and shallower vortices. Figure 8 also shows the time records from the two density probes indicating the changes of the density field during the break up process. The internal structures of the resulting two vortices can also be

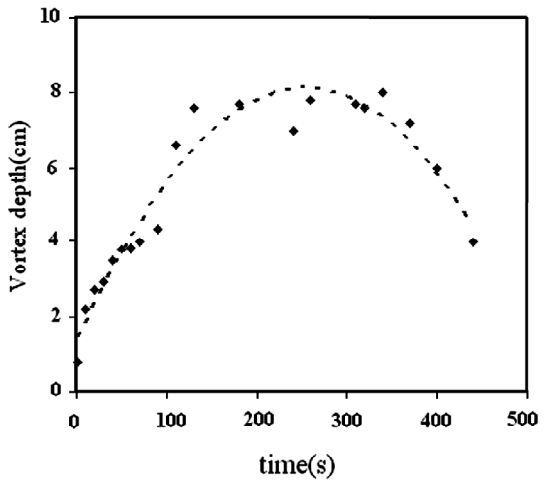

Figure 9. Time variations of the vortex depth (L_r=4.3 cm)

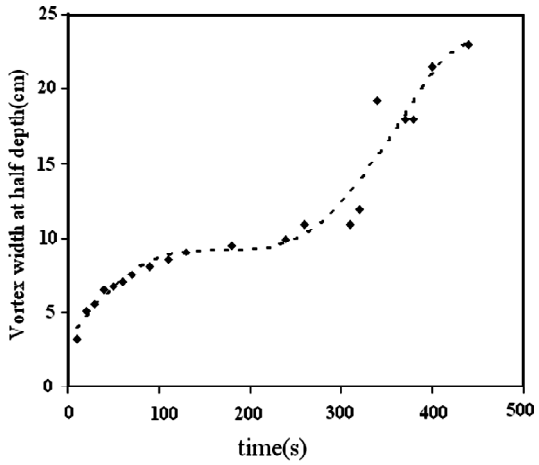

Figure 10. Time variations of the vortex half width (L_r=4.3 cm)

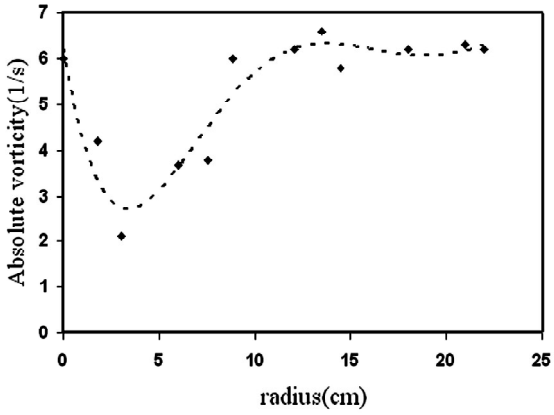

Figure 11. Absolute vorticity with respect to the radius of the vortex (L_r=4.3 cm)

inferred from the records. Further records of this kind can be found in Babaeian [15].

This is particularly the case as the radius of vortex becomes about 3.7 times that of Rossby radius of deformation of the environment. Baroclinic instability analysis of the flow predicts this at 3.9 L_r, which is close to this experimental finding. In each case, the Rossby radius of deformation (L_r =(g′H)$^{1/2}$/f) is distance in which a fluid parcel deflects 90° because of Coriolis force) and diameter of the vortex in the half width depth (L_v) of the vortex have been measured.

Time variations of the vortex depth, half width and absolute vorticity are found in the flow observations and are shown in Figures 9 to 11 [6 and 7]. These are for an experiment with L_r=4.3 cm. The growth of instability starts at about 360 s from the start of the experiment after which the depth of the vortex is substantially reduced while its size, which is now actually of two smaller vortices, increases by almost a factor of 2 or more. Absolute vorticity of the vortex is initially small as anticyclonic vorticity is induces during its initial formation. But as it breaks up, the flow acquires its initial absolute vorticity as the mixing of the vortex content occurs within the environment.

DISCUSION AND CONCLUSION

Two sets of experiments have been done to look at the ways structures of large scale Rossby waves and baroclinic vortices develop. The models are somewhat simple compared to the actual phenomena occurring in the atmosphere or ocean, but reveal in some qualitative way, features that are important in weather behavior or ozone hole formation in polar stratosphere [e. g. 9 and 10]. In the first set of experiments, we have simulated the formation of thermal Rossby waves in a rotating annulus using Rossby and Taylor numbers comparable to the ones for the atmosphere, but without beta effects (variation of f with latitude). The wave is superimposed on two opposing zonal jets (upper and lower). Introducing the beta effect by choosing sloping end walls at the top and bottom of the annulus creates further localized zonal jets [5]. Also in the

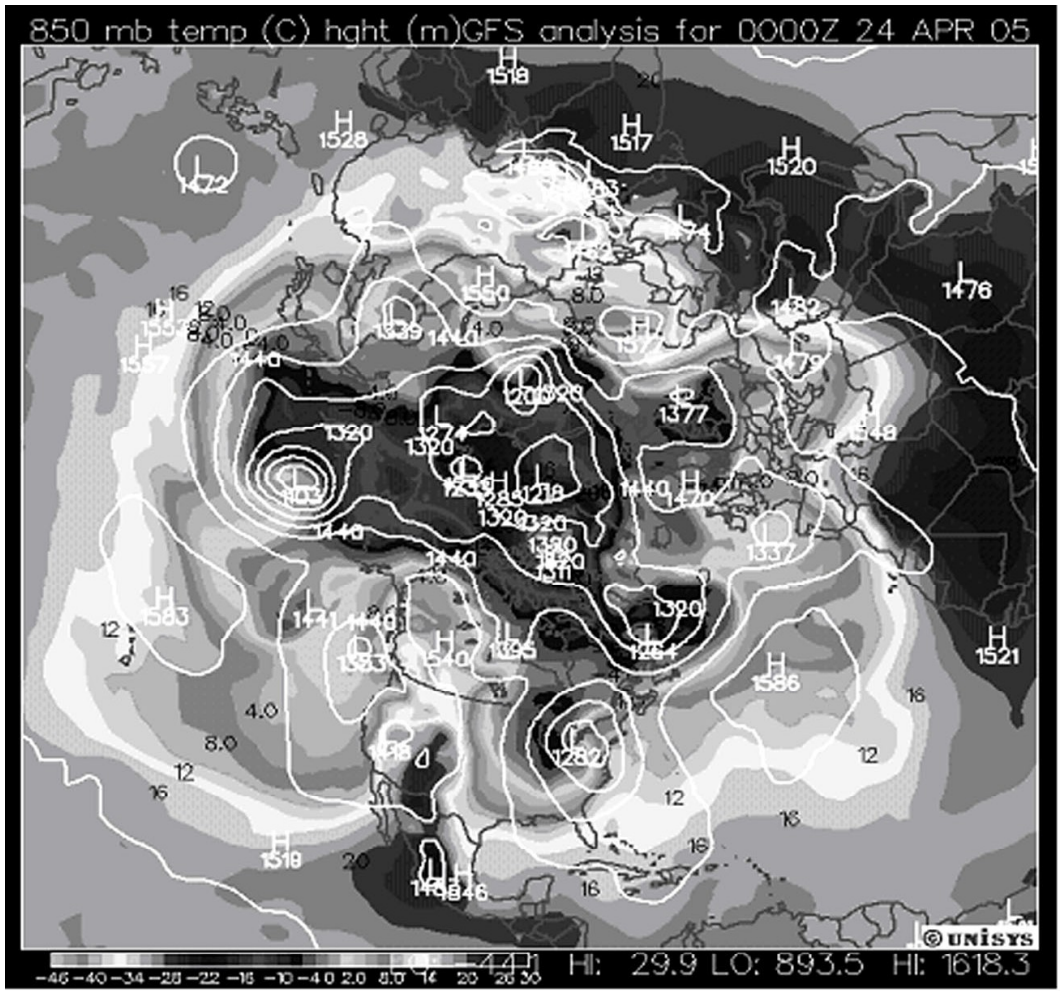

Figure 12. Geopotential heights (m) of 850 mb and the temperature field in the northern hemisphere. Cooler polar areas are colored blue [from UNIST web site].

Bastin and Read [5] experiment, the heating is internal (more applicable to atmosphere of giant plant) and not at the outer wall as in these experiment. In these experiments, we found that if $Ro_t \geq 0.4$ and $\tau \cong 1.3\times10^8$, the flow becomes unstable and irregular as usually the case for the atmosphere especially for the northern hemisphere as the land and water overages distribution is more complex. The meandering zonal jets encompasses baroclinic eddies on both sides known as cold and warm eddies. These eddies are clear in the present experiments, and are found to have well isolated cores [4]. Typical Rossby and Taylor numbers for the real atmosphere were estimated using 500 mb weather charts. The value of Ro_t was about 0.35 but τ is probably larger than that of these experiments and can not be estimated accurately with the weather charts data used here.

In the experiments of baroclinic vortex, which can be a model for polar stratospheric vortex, we found that the vortex became unstable, often with azimuthal wave number of 2 which turns it into an anticyclonic pair. Typically this occurs when the size of vortex (2R) is about the same as the 3.7 times the Rossby radius of deformation of the environment, as the baroclinic instability predicts. However, in real atmosphere, the break-down of vortices occurs at a range of 2 to 4 Rossby radii [8].The horizontal shear associated with the flow (which is barotropic) may restabilize the flow at larger scales as observed by Linden [6]. In addition to mode 2, instability with mode 1 (lateral displacement about the center of order of L_r) resulted as also been observed by Linden [6]. Since both of these instabilities are related to Rossby radius of the flow during these instabilities potential energy is released. This energy is fed to the kinetic energy of the mean flow, waves and smaller scale vortices. Fronts in rotating fluids, as the edge of the baroclinic vortex, can go unstable and generate smaller scale eddies which can lead to substantial cross-frontal buoyancy flux and mixing. Griffiths and Hopfinger [16] used laboratory experiments to find that the dispersion coefficient D of baroclinic eddies associated with baroclinic instability and their cross-frontal buoyancy flux B are given by:

$$D = 4g'H/f \tag{6}$$

and

$$B = (2g'H\delta\rho)/fW \tag{7}$$

where W is the width of the front which is in the order of the Rossby radius, and H is the depth of the frontal zone. Large scale fronts in the atmosphere and ocean as those associated with jet stream and Gulf Stream are unstable to the disturbances with wavelength of about 4 Rossby radii, which generate vortices such as those observed in the mid-latitudes. An example of such a complicated pattern of vortices is shown in Figure 12. The temperature field in this Figure. also follows the flow pattern. The vortices are in the order of the Rossby radius of the environment (about 1000 km for atmosphere). Such vortices determine how the weather evolves and affects our lives.

Thus, the present experiments reveal some of the observed features of the atmosphere only qualitatively, and can be used to understand some of the complex nonlinear processes involved in the real environments.

ACKNOWLEDGMENTS

All the laboratory experiments were performed at the Geophysical Fluid Dynamics Laboratory of the Geophysics Institute of Tehran University, the meteorological analyses were done at the National Institute of Climatology (NIC), Mashhad, Iran, to all of whom we are thankful.

REFERENCES

1. Hide R., "Rotating fluid in geophysics", Springer (London), (1980).
2. Hide R., *Dynamics of rotating fluid*, H. Roberts and A.M. Soward, (1978).
3. Hide R., "An experimental study of thermal convection in rotating liquid", *Q. J. Roy. Met. Soc*, **79**(161), (1958).
4. Tajma T., Nakamura T. and Sakata T., "Experimental observations of internal vortex structures in steady baroclinic waves", *J. Atmos. Sc*, **54**, PP 1600-1609(1997).
5. Bastin M. E. and Read P. I., "A laboratory study of baroclinic waves and turbulence in an internally hated fluid annulus with sloping end walls", PP 173-198(1997).
6. Linden P. F. , "Dynamics of fronts and eddies, in non-linear topics in ocean physics", *Italian Society of Physics*,, Summer School, Verona, Italy, (1988).
7. Hopfinger E. J. and Von-haijest , "Vortices in rotating fluid", *Ann. Rev. Fluid Mech*, **25**, PP 241-249(1993).
8. Bidokhti A.A. and Tritton, D. J. , "Experiments on turbulent free shear layers in rotating fluids.", *J. Fluid Mech*, PP 469-502(1992).
9. Holton J. R., *An introduction to dynamic meteorology*, (1992).
10. Turco R., *Earth under siege: From air pollution to global change*, 2Ed., Oxford University Press, (2002).
11. Brown R. A. , *Fluid mechanics of atmosphere*, (1991).
12. Dritshel D. G. and Legras B. , "Modeling oceanic and atmospheric vortices", *Physics Today (March)*, PP 44(1993).
13. Gill A. E., *Atmosphere ocean dynamics*, (1982).
14. Davies P. A. and Walin G., "Some exploratory experiments", *University of Stockholm, Rep.*, UDC-532, **52**, (1976).

15. Babaeian I., "Physical simulation of atmospheric baroclinic vortices.", M.Sc. Thesis, Geophysics Institute of Tehran University(1997).

16. Griffiths R. W. and Hopfinger E. J., "The structure of mesoscale turbulence and horizontal spreading at ocean fronts.", *Deep Sea Research*, **31**, PP 245-269(1984).